Viewing Graph Solvability via Cycle Consistency
Supplementary Material

Federica Arrigoni[1], Andrea Fusiello[2], Elisa Ricci[1,3] and Tomas Pajdla[4]
[1]University of Trento [2]University of Udine [3]Fondazione Bruno Kessler [4]CIIRC CTU in Prague
federica.arrigoni@unitn.it, andrea.fusiello@uniud.it, e.ricci@unitn.it, pajdla@cvut.cz

In this document we recall the most relevant equations related to our formulation, and we show how they look like on some examples, where we also analyze the output of our algorithm (Sec. 1). In addition, we report some visualization of the real experiments reported in the main paper (Sec. 2).

1. Examples

Let $\mathcal{G} = (\mathcal{V}, \mathcal{E})$ be a graph with n vertices and m edges, and let $\mathbf{c}_1, \dots, \mathbf{c}_n \in \mathbb{R}^4$ be n generic camera centres (e.g., sampled at random). Recall that sampling centres at random permits to check solvability in a generic sense, namely with cameras in a generic position, hence relying on the graph structure only. This is a standard procedure in solvability theory (see [7, 1]). Of course, there is a very small chance (with probability 0) to sample a degenerate configuration.

Let $\mathcal{L}(\mathcal{G}) = (\bar{\mathcal{V}}, \bar{\mathcal{E}})$ denote the line graph associated with $\mathcal{G}$. Viewing graph solvability [7] can be expressed as the problem of (uniquely) recovering an unknown matrix $G_\tau \in GL(4, \mathbb{R})$ for each node $\tau \in \bar{\mathcal{V}}$, in addition to an unknown vector $\mathbf{v}_{\tau\upsilon} \in \mathbb{R}^4$ and an unknown scale $a_{\tau\upsilon} \in \mathbb{R}_{\neq 0}$ for each edge $(\tau, \upsilon) \in \bar{\mathcal{E}}$, such that the following equation holds for all the edges in $\mathcal{L}(\mathcal{G})$:

$$G_\tau G_\upsilon^{-1} = Z_{\tau\upsilon} \tag{1}$$

where

$$Z_{\tau\upsilon} = a_{\tau\upsilon} I_4 + \mathbf{c}_i \mathbf{v}_{\tau\upsilon}^{\mathsf{T}}. \tag{2}$$

Recall that the index i of the camera is defined as $\{i\}=\tau\cap\upsilon$.

As shown in the main paper, the above system of equations can be equivalently expressed in terms of *cycle consistency*. Specifically, a *fundamental cycle basis* [4] (or, more generally, a *cycle consistency basis* [3]) for the line graph is considered, which is denoted by $\{\mathcal{C}_1, \dots, \mathcal{C}_k\}$, and equations of the following form are built for each cycle $\{\tau_1, \tau_2, \tau_3, \dots, \tau_\ell, \tau_1\}$ in the basis:

$$Z_{\tau_1\tau_2} Z_{\tau_2\tau_3} \cdot \dots \cdot Z_{\tau_\ell\tau_1} = I_4. \tag{3}$$

By exploiting a suitable a change of variables, Eq. (3) rewrites:

$$W_{\tau_1\tau_2} W_{\tau_2\tau_3} \cdot \dots \cdot W_{\tau_\ell\tau_1} = b_k I_4 \tag{4}$$

where $b_k \in \mathbb{R}_{\neq 0}$ is an unknown scale, $\mathbf{u}_{\tau\upsilon} \in \mathbb{R}^4$ is an unknown vector and $W_{\tau\upsilon}$ is defined by the following expression:

$$W_{\tau\upsilon} = I_4 + \mathbf{c}_i \mathbf{u}_{\tau\upsilon}^{\top}. \tag{5}$$

Finally, recall that an auxiliary equation of the following form is also considered for each edge in the line graph:

$$z_{\tau\upsilon} \det(I_4 + \mathbf{c}_i \mathbf{u}_{\tau\upsilon}^{\top}) + 1 = 0 \tag{6}$$

where $z_{\tau\upsilon} \in \mathbb{R}$ is an auxiliary variable. Equation (6) has the effect of automatically discarding non-invertible matrices and null scales from the solution set of our problem.

Hereafter, for a given edge $(\tau, \upsilon) \in \bar{\mathcal{E}}$ in the line graph – which corresponds to two adjacent edges in the original graph (i.e., $\tau = (h, i) \in \mathcal{E}$ and $\upsilon = (i, j) \in \mathcal{E}$) – we will use the triplet (h, i, j) instead of (τ, υ) for simplicity of exposition.

Example 1 (Non-solvable graph with infinite number of solutions). Suppose that $\mathcal{G}$ is a cycle of length 4, represented in Fig. 1. Let $\mathbf{c}_1, \mathbf{c}_2, \mathbf{c}_3, \mathbf{c}_4 \in \mathbb{R}^4$ represent known (generic) camera centres. Equation (1) rewrites

$$\begin{aligned} G_{12}G_{23}^{-1} &= a_{123}I_4 + \mathbf{c}_2\mathbf{v}_{123}^\mathsf{T} \\ G_{23}G_{34}^{-1} &= a_{234}I_4 + \mathbf{c}_3\mathbf{v}_{234}^\mathsf{T} \\ G_{34}G_{41}^{-1} &= a_{341}I_4 + \mathbf{c}_4\mathbf{v}_{341}^\mathsf{T} \\ G_{41}G_{12}^{-1} &= a_{412}I_4 + \mathbf{c}_1\mathbf{v}_{412}^\mathsf{T} \end{aligned} \tag{7}$$

where the following variables are unknown

$$\begin{gathered} G_{12}, G_{23}, G_{34}, G_{41} \in GL(4) \\ a_{123}, a_{234}, a_{341}, a_{412} \in \mathbb{R}_{\neq 0} \\ \mathbf{v}_{123}, \mathbf{v}_{234}, \mathbf{v}_{341}, \mathbf{v}_{412} \in \mathbb{R}^4. \end{gathered} \tag{8}$$

The line graph consists of a single cycle (of length 4), which is also a fundamental cycle basis (associated, e.g., with the spanning tree $\mathcal{T} = \{(12, 23), (23, 34), (34, 41)\}$), as shown in Fig. 1. Equation (3) rewrites

$$I_4 = (a_{123}I_4 + \mathbf{c}_2\mathbf{v}_{123}^\mathsf{T}) \cdot (a_{234}I_4 + \mathbf{c}_3\mathbf{v}_{234}^\mathsf{T}) \cdot (a_{341}I_4 + \mathbf{c}_4\mathbf{v}_{341}^\mathsf{T}) \cdot (a_{412}I_4 + \mathbf{c}_1\mathbf{v}_{412}^\mathsf{T}) \tag{9}$$

where the following variables are unknown

$$\begin{gathered} a_{123}, a_{234}, a_{341}, a_{412} \in \mathbb{R}_{\neq 0} \\ \mathbf{v}_{123}, \mathbf{v}_{234}, \mathbf{v}_{341}, \mathbf{v}_{412} \in \mathbb{R}^4. \end{gathered} \tag{10}$$

Equation (4) rewrites

$$bI_4 = (I_4 + \mathbf{c}_2\mathbf{u}_{123}^\mathsf{T}) \cdot (I_4 + \mathbf{c}_3\mathbf{u}_{234}^\mathsf{T}) \cdot (I_4 + \mathbf{c}_4\mathbf{u}_{341}^\mathsf{T}) \cdot (I_4 + \mathbf{c}_1\mathbf{u}_{412}^\mathsf{T}) \tag{11}$$

where the following variables are unknown

$$\begin{gathered} b \in \mathbb{R}_{\neq 0} \\ \mathbf{u}_{123}, \mathbf{u}_{234}, \mathbf{u}_{341}, \mathbf{u}_{412} \in \mathbb{R}^4. \end{gathered} \tag{12}$$

Observe that Eq. (11) involves less unknowns than (9), which in turn involves less unknowns than (7), as already observed in the main paper. Finally, the auxiliary equations given in (6) become

$$\begin{aligned} z_{123} \det(I_4 + \mathbf{c}_2\mathbf{u}_{123}^\mathsf{T}) + 1 = 0 \\ z_{234} \det(I_4 + \mathbf{c}_3\mathbf{u}_{234}^\mathsf{T}) + 1 = 0 \\ z_{341} \det(I_4 + \mathbf{c}_4\mathbf{u}_{341}^\mathsf{T}) + 1 = 0 \\ z_{412} \det(I_4 + \mathbf{c}_1\mathbf{u}_{412}^\mathsf{T}) + 1 = 0 \end{aligned} \tag{13}$$

where $z_{123}, z_{234}, z_{341}, z_{412} \in \mathbb{R}$ are unknown.

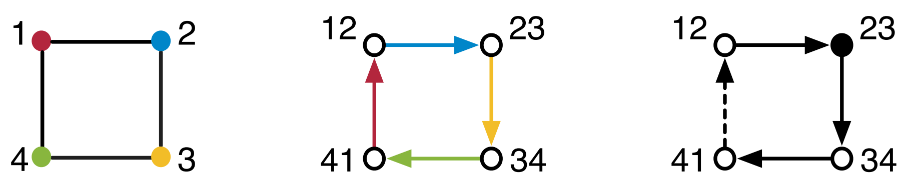

Figure 1: Non-solvable viewing graph with 4 vertices (left) and corresponding line graph (middle), where edges are oriented arbitrarily. Colors clarify correspondences between edges in the line graph and vertices in the original graph. On the right a spanning tree is reported, where the root is coloured in black and the only non-tree edge is drawn with a dashed arrow.

The fact that the graph in Fig. 1 is not solvable can be easily deduced by counting the number of edges: the necessary condition $m \geqslant (11n-15)/7$ is not satisfied here (see [7]). However, it is useful to analyze the output of our algorithm on this simple example. Specifically, Fig. 2 shows the generators of the Gröbner basis [2] associated with the polynomial system in Eq. (11) and (13), for a specific configuration of camera centers (sampled at random). Such generators encode a set of equations which is equivalent to the original system but at the same time it is much simpler. Let us consider the last generator (i.e. $\mathtt{z\_2z\_3}-1=0$): note that the product of $\mathtt{z\_2}$ and $\mathtt{z\_3}$ is fixed (it is equal to 1), but there is an *infinite* number of solutions that satisfy such equation. Observe also that the remaining variables are uniquely determined – given $\mathtt{z\_2}$ and $\mathtt{z\_3}$ – as all other equations are linear and they involve one unknown at a time (in addition to $\mathtt{z\_2}$ or $\mathtt{z\_3}$).

```
z_1-z_3, z_0-z_2, u_15-559z_2-559, u_14-10838z_3-10838, u_13+7287z_2+7287, u_12-7283z_3-7283, u_11+7762z_2+7762, u_10-12207z_3-12207,
u_9-12548z_2-12548, u_8-7348z_3-7348, u_7-14623z_2-14623, u_6-6734z_3-6734, u_5+11215z_2+11215, u_4-2201z_3-2201, u_3-4301z_2-4301,
u_2+14484z_3+14484, u_1+11757z_2+11757, u_0-11403z_3-11403, b_0+z_3, z_2z_3-1
```

Figure 2: Gröbner basis associated with the polynomial system in Eq. (11) and (13), for a specific set of camera centres. For coherence with our Macaulay2 implementation, here variables are linearly (0-based) indexed. Each term represents a polynomial which should be equal to zero for the sought solution(s).

Example 2 (Non-solvable graph with finite number of solutions). The previous example refers to a non-solvable graph with an infinite number of solutions. We now consider an example of a non-solvable graph where the number of solutions is finite but strictly greater than one. Specifically, let us consider the graph with 9 nodes reported in Fig. 5 (left) of the main paper. Our algorithm computed two solutions on this example, meaning that the graph is not solvable. Since a lot of variables are involved here, we do not explicitly write all the equations for this example, but we only analyze the associated Gröbner basis obtained for a specific configuration of random cameras (see Fig. 3). Let us consider the last generator (i.e., $\mathtt{z\_20\hat{}2} - 4598\mathtt{z\_20} - 4599 = 0$): observe that it defines an equation of degree two in one unknown. Observe also that all other equations are linear and they involve one unknown at a time (in addition to $\mathtt{z\_20}$). Since we know that one of the solutions is $\mathtt{z\_20} = -1$, we see that the other solution for $\mathtt{z\_20}$ has to be real as well (namely $\mathtt{z\_20} = 4599$). Thus, all other variables have to be real too, since they are linear functions of $\mathtt{z\_20}$. Hence, the whole polynomial system admits two distinct real solutions.

```
z_19+12604z_20+12605, z_18-11727z_20-11726, z_17+894z_20+895, z_16-z_20, z_15-3343z_20-3342, z_14+894z_20+895, z_13+11565z_20+11566,
z_12-13791z_20-13790, z_11+8203z_20+8204, z_10-8522z_20-8521, z_9+7215z_20+7216, z_8-1877z_20-1876, z_7-11118z_20-11117, z_6-7063z_20-7062,
z_5-7412z_20-7411, z_4+8437z_20+8438, z_3+1796z_20+1797, z_2+5030z_20+5031, z_1-2848z_20-2847, z_0-9253z_20-9252, u_83-8414z_20-8414,
u_82+10987z_20+10987, u_81-3919z_20-3919, u_80+973z_20+973, u_79-10847z_20-10847, u_78-5390z_20-5390, u_77+431z_20+431, u_76-13455z_20-13455,
u_75-3615z_20-3615, u_74+3100z_20+3100, u_73-9420z_20-9420, u_72-10243z_20-10243, u_71+4517z_20+4517, u_70+1766z_20+1766, u_69+6198z_20+6198,
u_68+681z_20+681, u_67-7149z_20-7149, u_66-2977z_20-2977, u_65+11405z_20+11405, u_64-3437z_20-3437, u_63-7836z_20-7836, u_62+13583z_20+13583,
u_61+1799z_20+1799, u_60-8356z_20-8356, u_59-10495z_20-10495, u_58-9989z_20-9989, u_57+9771z_20+9771, u_56+12865z_20+12865, u_55+10476z_20+10476,
u_54-13684z_20-13684, u_53-14439z_20-14439, u_52-6145z_20-6145, u_51-11189z_20-11189, u_50-3733z_20-3733, u_49+10275z_20+10275, u_48-4355z_20-4355,
u_47+14504z_20+14504, u_46+13506z_20+13506, u_45+10191z_20+10191, u_44-1472z_20-1472, u_43+6220z_20+6220, u_42+9716z_20+9716, u_41-66z_20-66,
u_40+2077z_20+2077, u_39+9070z_20+9070, u_38+603z_20+603, u_37-7509z_20-7509, u_36-12738z_20-12738, u_35-10638z_20-10638, u_34+1764z_20+1764,
u_33-9009z_20-9009, u_32-8517z_20-8517, u_31+8333z_20+8333, u_30+1020z_20+1020, u_29-10090z_20-10090, u_28-14978z_20-14978, u_27-13238z_20-13238,
u_26-941z_20-941, u_25-13990z_20-13990, u_24-11470z_20-11470, u_23-14044z_20-14044, u_22-1292z_20-1292, u_21+1034z_20+1034, u_20-4116z_20-4116,
u_19-1995z_20-1995, u_18-14930z_20-14930, u_17+3697z_20+3697, u_16-10633z_20-10633, u_15-900z_20-900, u_14+458z_20+458, u_13+5440z_20+5440,
u_12-11618z_20-11618, u_11-2465z_20-2465, u_10-247z_20-247, u_9-10781z_20-10781, u_8-6754z_20-6754, u_7-4883z_20-4883, u_6-6092z_20-6092,
u_5+5548z_20+5548, u_4-2399z_20-2399, u_3-4745z_20-4745, u_2-3226z_20-3226, u_1-5879z_20-5879, u_0-1620z_20-1620, b_9-1, b_8+6278z_20+6277, b_7-1,
b_6+11118z_20+11117, b_5+7063z_20+7062, b_4+7167z_20+7166, b_3-1, b_2+8994z_20+8993, b_1-1, b_0-1, z_20^2-4598z_20-4599
```

Figure 3: Gröbner basis for checking solvability for the graph in Fig. 5 (left) of the main paper. For coherence with our Macaulay2 implementation, here variables are linearly (0-based) indexed. Each term represents a polynomial which should be equal to zero for the sought solution(s).

Example 3 (Solvable graph). Suppose that $\mathcal{G}$ is the graph reported in Fig. 4. Let $\mathbf{c}_1, \mathbf{c}_2, \mathbf{c}_3, \mathbf{c}_4 \in \mathbb{R}^4$ represent known (generic) camera centres. Equation (1) rewrites

$$\begin{aligned}
G_{41}G_{12}^{-1} &= a_{412}I_4 + \mathbf{c}_1\mathbf{v}_{412}^{\mathsf{T}} \\
G_{12}G_{23}^{-1} &= a_{123}I_4 + \mathbf{c}_2\mathbf{v}_{123}^{\mathsf{T}} \\
G_{23}G_{34}^{-1} &= a_{234}I_4 + \mathbf{c}_3\mathbf{v}_{234}^{\mathsf{T}} \\
G_{34}G_{41}^{-1} &= a_{341}I_4 + \mathbf{c}_4\mathbf{v}_{341}^{\mathsf{T}} \\
G_{12}G_{42}^{-1} &= a_{124}I_4 + \mathbf{c}_2\mathbf{v}_{124}^{\mathsf{T}} \\
G_{42}G_{23}^{-1} &= a_{423}I_4 + \mathbf{c}_2\mathbf{v}_{423}^{\mathsf{T}} \\
G_{41}G_{42}^{-1} &= a_{142}I_4 + \mathbf{c}_4\mathbf{v}_{142}^{\mathsf{T}} \\
G_{42}G_{34}^{-1} &= a_{243}I_4 + \mathbf{c}_4\mathbf{v}_{243}^{\mathsf{T}}
\end{aligned} \tag{14}$$

where the following variables are unknown

$$\begin{gathered}
G_{12}, G_{23}, G_{34}, G_{41}, G_{42} \in GL(4) \\
a_{412}, a_{123}, a_{234}, a_{341}, a_{124}, a_{423}, a_{142}, a_{243} \in \mathbb{R}_{\neq 0} \\
\mathbf{v}_{412}, \mathbf{v}_{123}, \mathbf{v}_{234}, \mathbf{v}_{341}, \mathbf{v}_{124}, \mathbf{v}_{423}, \mathbf{v}_{142}, \mathbf{v}_{243} \in \mathbb{R}^4.
\end{gathered} \tag{15}$$

If we consider the spanning tree $\mathcal{T} = \{(12, 42), (42, 23), (42, 34), (42, 41)\}$, then the line graph admits a fundamental cycle basis composed of four cycles (see Fig. 4): $\mathcal{C}_1 = (12, 23, 42)$, $\mathcal{C}_2 = (42, 23, 34)$, $\mathcal{C}_3 = (42, 34, 41)$ and $\mathcal{C}_4 = (41, 12, 42)$. Observe that each cycle consists of a sequence of vertices that is traversed in a cyclic order (clockwise or anticlockwise): for each edge in the cycle, we consider the associated matrix or its inverse if the edge is traversed in forward or backward direction, respectively. Thus Eq. (3) becomes

$$\begin{aligned}
I_4 &= (a_{123}I_4 + \mathbf{c}_2\mathbf{v}_{123}^{\mathsf{T}}) \cdot (a_{423}I_4 + \mathbf{c}_2\mathbf{v}_{423}^{\mathsf{T}})^{-1} \cdot (a_{124}I_4 + \mathbf{c}_2\mathbf{v}_{124}^{\mathsf{T}})^{-1} \\
I_4 &= (a_{423}I_4 + \mathbf{c}_2\mathbf{v}_{423}^{\mathsf{T}}) \cdot (a_{234}I_4 + \mathbf{c}_3\mathbf{v}_{234}^{\mathsf{T}}) \cdot (a_{243}I_4 + \mathbf{c}_4\mathbf{v}_{243}^{\mathsf{T}})^{-1} \\
I_4 &= (a_{243}I_4 + \mathbf{c}_4\mathbf{v}_{243}^{\mathsf{T}}) \cdot (a_{341}I_4 + \mathbf{c}_4\mathbf{v}_{341}^{\mathsf{T}}) \cdot (a_{142}I_4 + \mathbf{c}_4\mathbf{v}_{142}^{\mathsf{T}}) \\
I_4 &= (a_{412}I_4 + \mathbf{c}_1\mathbf{v}_{412}^{\mathsf{T}}) \cdot (a_{124}I_4 + \mathbf{c}_2\mathbf{v}_{124}^{\mathsf{T}}) \cdot (a_{142}I_4 + \mathbf{c}_4\mathbf{v}_{142}^{\mathsf{T}})^{-1}
\end{aligned} \tag{16}$$

where the following variables are unknown

$$\begin{gathered}
a_{412}, a_{123}, a_{234}, a_{341}, a_{124}, a_{423}, a_{142}, a_{243} \in \mathbb{R}_{\neq 0} \\
\mathbf{v}_{412}, \mathbf{v}_{123}, \mathbf{v}_{234}, \mathbf{v}_{341}, \mathbf{v}_{124}, \mathbf{v}_{423}, \mathbf{v}_{142}, \mathbf{v}_{243} \in \mathbb{R}^4.
\end{gathered} \tag{17}$$

Equation (4) rewrites

$$\begin{aligned}
b_1 I_4 &= (I_4 + \mathbf{c}_2\mathbf{u}_{123}^{\mathsf{T}}) \cdot (I_4 + \mathbf{c}_2\mathbf{u}_{423}^{\mathsf{T}})^{-1} \cdot (I_4 + \mathbf{c}_2\mathbf{u}_{124}^{\mathsf{T}})^{-1} \\
b_2 I_4 &= (I_4 + \mathbf{c}_2\mathbf{u}_{423}^{\mathsf{T}}) \cdot (I_4 + \mathbf{c}_3\mathbf{u}_{234}^{\mathsf{T}}) \cdot (I_4 + \mathbf{c}_4\mathbf{u}_{243}^{\mathsf{T}})^{-1} \\
b_3 I_4 &= (I_4 + \mathbf{c}_4\mathbf{u}_{243}^{\mathsf{T}}) \cdot (I_4 + \mathbf{c}_4\mathbf{u}_{341}^{\mathsf{T}}) \cdot (I_4 + \mathbf{c}_4\mathbf{u}_{142}^{\mathsf{T}}) \\
b_4 I_4 &= (I_4 + \mathbf{c}_1\mathbf{u}_{412}^{\mathsf{T}}) \cdot (I_4 + \mathbf{c}_2\mathbf{u}_{124}^{\mathsf{T}}) \cdot (I_4 + \mathbf{c}_4\mathbf{u}_{142}^{\mathsf{T}})^{-1}
\end{aligned} \tag{18}$$

where the following variables are unknown

$$\begin{gathered}
b_1, b_2, b_3, b_4 \in \mathbb{R}_{\neq 0} \\
\mathbf{u}_{412}, \mathbf{u}_{123}, \mathbf{u}_{234}, \mathbf{u}_{341}, \mathbf{u}_{124}, \mathbf{u}_{423}, \mathbf{u}_{142}, \mathbf{u}_{243} \in \mathbb{R}^4.
\end{gathered} \tag{19}$$

Observe that the formulation implemented by our method (given in Eq. (18)) involves less unknowns than the one proposed in [7] (given in Eq. (14)). By computing inverses explicitly[1], Eq. (18) rewrites:

$$\begin{aligned}
(1 + \mathbf{c}_2^{\mathsf{T}}\mathbf{u}_{423})(1 + \mathbf{c}_2^{\mathsf{T}}\mathbf{u}_{124})b_1 I_4 &= (I_4 + \mathbf{c}_2\mathbf{u}_{123}^{\mathsf{T}}) \cdot ((1 + \mathbf{c}_2^{\mathsf{T}}\mathbf{u}_{423})I_4 - \mathbf{c}_2\mathbf{u}_{423}^{\mathsf{T}}) \cdot ((1 + \mathbf{c}_2^{\mathsf{T}}\mathbf{u}_{124})I_4 - \mathbf{c}_2\mathbf{u}_{124}^{\mathsf{T}}) \\
(1 + \mathbf{c}_4^{\mathsf{T}}\mathbf{u}_{243})b_2 I_4 &= (I_4 + \mathbf{c}_2\mathbf{u}_{423}^{\mathsf{T}}) \cdot (I_4 + \mathbf{c}_3\mathbf{u}_{234}^{\mathsf{T}}) \cdot ((1 + \mathbf{c}_4^{\mathsf{T}}\mathbf{u}_{243})I_4 - \mathbf{c}_4\mathbf{u}_{243}^{\mathsf{T}}) \\
b_3 I_4 &= (I_4 + \mathbf{c}_4\mathbf{u}_{243}^{\mathsf{T}}) \cdot (I_4 + \mathbf{c}_4\mathbf{u}_{341}^{\mathsf{T}}) \cdot (I_4 + \mathbf{c}_4\mathbf{u}_{142}^{\mathsf{T}}) \\
(1 + \mathbf{c}_4^{\mathsf{T}}\mathbf{u}_{142})b_4 I_4 &= (I_4 + \mathbf{c}_1\mathbf{u}_{412}^{\mathsf{T}}) \cdot (I_4 + \mathbf{c}_2\mathbf{u}_{124}^{\mathsf{T}}) \cdot ((1 + \mathbf{c}_4^{\mathsf{T}}\mathbf{u}_{142})I_4 - \mathbf{c}_4\mathbf{u}_{142}^{\mathsf{T}})
\end{aligned} \tag{20}$$

[1] The inverse of a matrix of the form $I_4 + \mathbf{c}\mathbf{u}^{\mathsf{T}}$ is given by $I_4 + \mathbf{c}\mathbf{w}^{\mathsf{T}}$ where $\mathbf{w} = -\frac{1}{1+\mathbf{c}^{\mathsf{T}}\mathbf{u}}\mathbf{u}$.

Finally, the auxiliary equations given in (6) become

$$
\begin{aligned}
z_{412}\det(I_4+\mathbf{c}_1\mathbf{u}_{412}^{\mathsf{T}})+1&=0\\
z_{123}\det(I_4+\mathbf{c}_2\mathbf{u}_{123}^{\mathsf{T}})+1&=0\\
z_{234}\det(I_4+\mathbf{c}_3\mathbf{u}_{234}^{\mathsf{T}})+1&=0\\
z_{341}\det(I_4+\mathbf{c}_4\mathbf{u}_{341}^{\mathsf{T}})+1&=0\\
z_{124}\det(I_4+\mathbf{c}_2\mathbf{u}_{124}^{\mathsf{T}})+1&=0\\
z_{423}\det(I_4+\mathbf{c}_2\mathbf{u}_{423}^{\mathsf{T}})+1&=0\\
z_{142}\det(I_4+\mathbf{c}_4\mathbf{u}_{142}^{\mathsf{T}})+1&=0\\
z_{243}\det(I_4+\mathbf{c}_4\mathbf{u}_{243}^{\mathsf{T}})+1&=0
\end{aligned}
\tag{21}
$$

where $z_{412}, z_{123}, z_{234}, z_{341}, z_{124}, z_{423}, z_{142}, z_{243} \in \mathbb{R}$ are unknown.

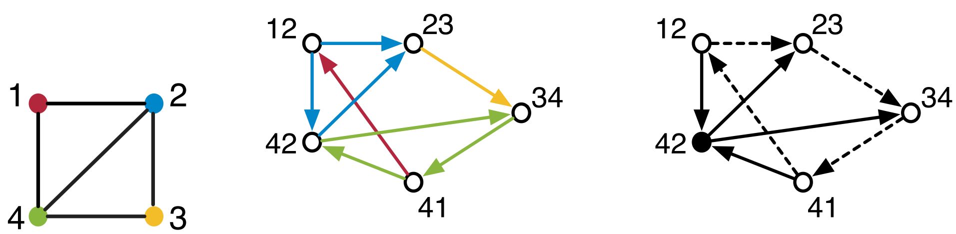

Figure 4: Solvable viewing graph with 4 vertices (left) and corresponding line graph (middle), where edges are oriented arbitrarily. Please note that a vertex of the original graph (e.g., vertex 2) can appear multiple times as an edge of the line graph, as clarified by colors. On the right a spanning tree is reported, where the root is coloured in black and non-tree edges are drawn with dashed arrows.

The graph in Fig. 4 is solvable according to [5] and our algorithm returns exactly one solution. Such conclusion can also be easily deduced from Fig. 5, which reports the generators of the Gröbner basis associated with the polynomial system in Eq. (20) and (21). Observe that each generator has exactly one solution, being a linear equation in one variable. In particular, we get $\mathtt{z\_0} = \mathtt{z\_1} = \cdots = \mathtt{z\_7} = -1$, $\mathtt{b\_0} = \mathtt{b\_1} = \mathtt{b\_2} = \mathtt{b\_3} = 1$ and $\mathtt{u\_0} = \mathtt{u\_1} = \cdots = \mathtt{u\_31} = 0$, as expected for a solvable graph.

```
z_7+1, z_6+1, z_5+1, z_4+1, z_3+1, z_2+1, z_1+1, z_0+1, u_31, u_30, u_29, u_28, u_27, u_26, u_25, u_24, u_23, u_22, u_21, u_20, u_19, u_18, u_17,
u_16, u_15, u_14, u_13, u_12, u_11, u_10, u_9, u_8, u_7, u_6, u_5, u_4, u_3, u_2, u_1, u_0, b_3-1, b_2-1, b_1-1, b_0-1
```

Figure 5: Gröbner basis associated with the polynomial system in Eq. (20) and (21), for a specific set of camera centres. For coherence with our Macaulay2 implementation, here variables are linearly (0-based) indexed. Each term represents a polynomial which should be equal to zero for the sought solution.

2. Visual Results

In this section we report some visual results associated with the real experiments reported in the main paper, where small subgraphs (with 9 nodes) were sampled from large graphs appearing in real datasets. Figure 6 shows some unsolvable cases whereas Fig. 7 reports some solvable examples.

References

[1] F. Arrigoni and A. Fusiello. Bearing-based network localizability: A unifying view. *IEEE Transactions on Pattern Analysis and Machine Intelligence*, 41(9):2049 – 2069, 2019. 1

[2] T. W. Dubé. The structure of polynomial ideals and Gröbner bases. *SIAM Journal on Computing*, 19(4):750 – 773, 1990. 3

[3] L. J. Guibas, Q. Huang, and Z. Liang. A condition number for joint optimization of cycle-consistent networks. In *Neural Information Processing Systems*, volume 32, pages 1007–1017, 2019. 1

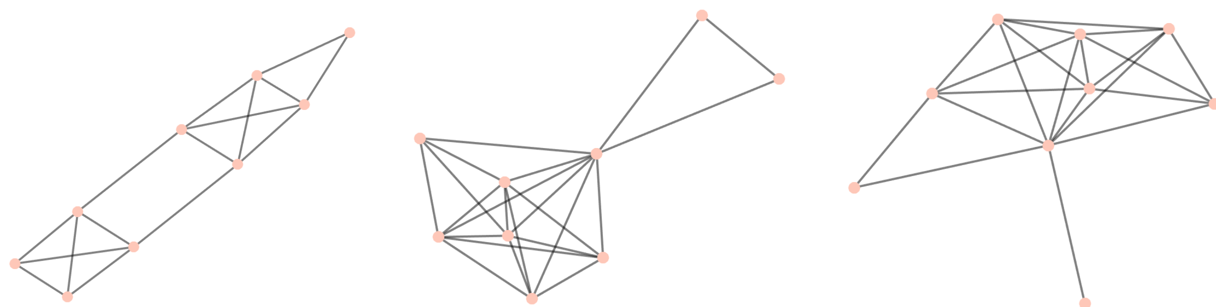

Figure 6: Examples of unsolvable sub-graphs with nine nodes sampled from the viewing graph of the Pumpkin data set [6].

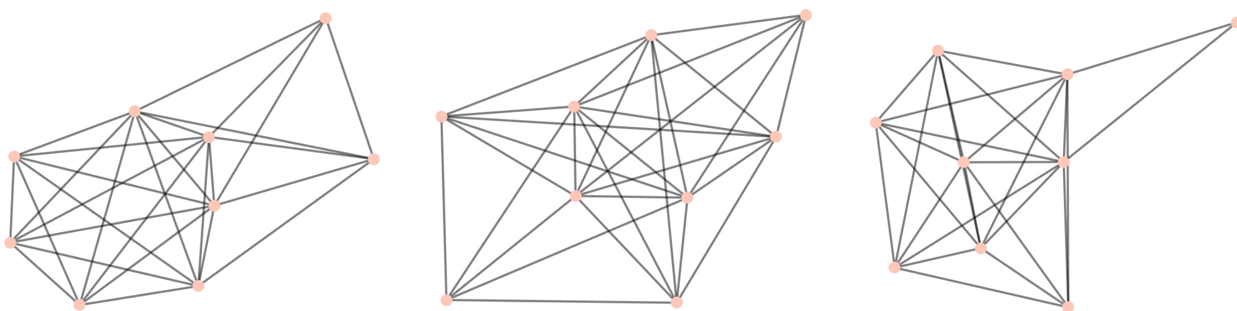

Figure 7: Examples of solvable sub-graphs with nine nodes sampled from the viewing graph of the Pumpkin data set [6].

[4] T. Kavitha, C. Liebchen, K. Mehlhorn, D. Michail, R. Rizzi, T. Ueckerdt, and K. Zweig. Cycle bases in graphs: Characterization, algorithms, complexity, and applications. *Computer Scienze Review*, 3(4):199–243, 2009. 1

[5] N. Levi and M. Werman. The viewing graph. In *Proceedings of the IEEE Conference on Computer Vision and Pattern Recognition*, pages 518 – 522, 2003. 5

[6] C. Olsson and O. Enqvist. Stable structure from motion for unordered image collections. In *Proceedings of the 17th Scandinavian conference on Image analysis (SCIA'11)*, pages 524–535. Springer-Verlag, 2011. 6

[7] M. Trager, B. Osserman, and J. Ponce. On the solvability of viewing graphs. In *Proceedings of the European Conference on Computer Vision*, pages 335–350, 2018. 1, 3, 4